2009 International Conference on Machine Learning and Computing
IPCSIT vol.3 (2011) © (2011) IACSIT Press, Singapore

A Novel Model-based Predictive Wavelet Network Strategy for Control of Spark Injection Engines

Javad Abdi [1], Hossein Ahmadi Noubari [2, 3], Hossein Borhanifar [1]

[1] Department of Electrical and Computer Engineering, Islamic Azad University, NazarAbad Branch, Iran
[2] Department of Electrical & Computer Engineering, University of Tehran, Tehran, Iran
[3] Department of Electrical & Computer Engineering, University of British Colombia, Canada

Abstract. An application of wavelet neural network/wavenet in control problems of nonlinear systems is investigated in this study. A wavelet neural network is constructed as an alternative architecture to a neural network to approximate a nonlinear system. Based on approximation capability of wavelet network, a suitable adaptive control law and parameter updating algorithm as applied to nonlinear system uncertainty estimation are developed. It is shown that using wavelet neural networks, an effective uncertainty estimation and control strategy can be obtained. This method improves plant performance effectively and provides robustness against variations caused by changes in operating points of the system. Simulation results show the superiority of the method.

Keywords: Wavelet neural network (WNN), A/F ratio, SI engines, NN, Estimator, Internal combustion

1. Introduction

During the last two decades, engine exhaust control problem has been under study by different research groups as well as by automobile industry [6, 7, 8, and 9].

Control of the A/F ratio using catalyst converters has been shown to be an effective alternative for the reduction of emission rate of noxious gases such as CO, HC and NOx in SI engines. However due to the presence of uncertainty in plant models as well as time delays and the parameter variations caused by changes in operating point of the engine or environment conditions, an accurate control of the A/F ratio is not always possible. Some of the solutions alternatives cope for this problem are based on using maps of engine bed tests derived for the entire range of operating points. For example, in fuzzy control methods, these maps are applied extensively [6]. The solutions to this problem are based on the estimation theory that utilizes identification techniques to determine engine parameter values. However, because of the noise effect and the rapidly changing engine work point even in extended techniques, the estimated parameter values will be associated with considerable error [1, 2]. While using nonlinear methods such as sliding mode, may improve the results, however due to the presence of delay and noise in the plant, unwanted oscillations may occur [7, 6]. In this paper we will attempt to use wavelet neural network to model the dynamics of the system and to determine an optimum A/F ratio. The method is considered to be a popular control approach to control A/F ratio due to its capability to learn plant model by using, inverse plant maps and uncertain factors in plants [5]. Wavelet neural networks or wavelet networks are the neural networks in which the activation functions are considered to be wavelet basic functions (e.g., sigmoid, Morlet, etc.). Nevertheless because of the delay and parameter variations in work point space, this method doesn't guarantee precise and rapid response [8, 9]. In this paper, our analysis will start with the introduction of plant model in section 2 followed by the use of both wavelet neural network and controller using sigmoid activation functions. The structure of the controller will be discussed in section 3. Simulation results will be provided in section 4.

2. An Applied model

The air-fuel ratio control operation can be described as mixing of air mass that is regulated as a function of the throttle valve angle excited. It is done by the driver and the engine speed; with a fuel mass that is injected by the electromagnetic nuzzle as the main actuator.

2.1. Air flow dynamics

Manifold pressure, which is dependent on the throttle valve angle, and engine speed are the main factors that determine quantity of air mass entering into the cylinder. Some other less prominent factors such as environmental conditions and manifold geometry, contribute also to the air mass flow rate.

If the rate of the air mass flow were measurable at the combustion inlet, computing the airflow mass would then be possible. Therefore, most designers prefer to use a prepared map derived from the work point space for measurement of air mass flow by testing motor. Here, we assume that, m_a, the intake air mass, enters into the cylinder at each cycle which is a function of the engine speed n_{rpm} and the throttle angle α [10].

$$m_a = m_a(\alpha, n_{rpm}) \tag{1}$$

2.2. Fuel flow dynamics

Because of wall wetting, a portion of the fuel mass is deposited on the wall of inlet pipe. As a result, when an increase or a decrease of engine speed occurs, the A/F ratio would be rich or lean. Because of the engine heat and the ambient temperature, a fraction of this puddle fuel vaporizes and flows into the cylinder.

Since model parameters vary with work point [1], a dynamic model for wall wetting is considered as follows. .

$$m_{fp}(k+1) = (1-f_\beta)*m_{fp}(k) + (1-f_\alpha)*m_{fi}(k) \tag{2}$$

$$m_f(k) = f_\beta * m_{fp}(k) + f_\alpha * m_{fi}(k) \tag{3}$$

where k: Engine cycle index (1 cycle=720^o crank)

m_{fp}: Liquid fuel puddle mass m_f: Fuel mass into the cylinder per cycle

m_{fi}: Fuel mass injected f_α: Fraction of injected fuel that enters the cylinder directly each cycle

f_β: Fraction of fuel puddle that evaporates and enters the cylinder each cycle

2.3. Time delay and measurement dynamics

The mixture of A/F that enters into the combustion chamber during the intake stroke is compressed and is ignited at the fourth stroke. It then, is transferred from the outlet manifold to the exhaust pipe, hence reaching the EGO sensor. Two types of time delays are defined during this gas transfer. The first delay belongs to time difference between the time of the entrance of the gas mixture into intake manifold and the time of the combusted gas reaching the outlet manifold. This delay varies inversely with the engine speed.

$T = 120/(n*cyl)$ (s)

where n: is engine revolution per minute and cyl: is the number of cylinders (In this paper we consider $cyl = 1$ however, the results would be extended easily to other cases.) The second delay τ_d occurs during the gas transfer from outlet manifold to the position of the sensor. Assuming the plug flow in the exhaust manifold, then the average velocity of the exhaust gases will be proportional to the engine speed. Thus the transport delay varies inversely with the engine speed because of proximity of EGO sensor to exhaust valve and noting that the blast off exhaust gases during the blow down process dominates time delay, τ_d which varies with both dimensions of work point. The sampling rate being based on the crank angle, the modified equation will be as follows. [1]: $\phi_m(k+1) = \gamma_0\phi_m(k) + \gamma_1\phi_c(k) + \gamma_2\phi_e(k)$ (4)

where: ϕ_c: A/F ratio from gas that goes into the cylinder, ϕ_e: A/F ratio from gas that goes out of the outlet manifold, ϕ_m: The signal measured by the sensor

and

$$\gamma_0 = e^{-\frac{T}{\tau_e}},\quad \gamma_1 = e^{-\frac{mT}{\tau_e}} - e^{-\frac{T}{\tau_e}},\quad \gamma_2 = 1 - e^{-\frac{mT}{\tau_e}}$$

where: τ_e is a time constant for the sensor and $m = 2 - \tau_d / T$.

Finally considering equations (1) to (4) the overall plant state equations are:

$$\underbrace{\begin{bmatrix} m_{fp} \\ \phi_e \\ \phi_d \\ \phi_m \end{bmatrix}_{K+1}}_{X_{K+1}} = \underbrace{\begin{bmatrix} 1-f_\beta & 0 & 0 & 0 \\ \frac{\lambda_s}{\overline{m}_a} f_\beta & 0 & 0 & 0 \\ 0 & 1 & 0 & 0 \\ 0 & \gamma_2 & \gamma_1 & \gamma_0 \end{bmatrix}_K}_{G} \underbrace{\begin{bmatrix} m_{fp} \\ \phi_e \\ \phi_d \\ \phi_m \end{bmatrix}_k}_{X_k} + \underbrace{\begin{bmatrix} 1-f_\alpha \\ \frac{\lambda_s}{\overline{m}_a} f_\alpha \\ 0 \\ 0 \end{bmatrix}_k}_{H} \underbrace{\left[\overline{m}_{fi}\right]_k}_{u_k} \quad (5) \quad \underbrace{\phi_m|_k}_{y_k} = \underbrace{\begin{bmatrix} 0 & 0 & 0 & 1 \end{bmatrix}}_{C} \underbrace{\begin{bmatrix} m_{fp} \\ \phi_e \\ \phi_d \\ \phi_m \end{bmatrix}_k}_{X_k} \quad (6)$$

where $\lambda_s = 14.7$ is the stochiometric A/F ratio.

Almost all physical parameters vary with work point dimensions or engine speed and throttle valve angle. In this paper, we attempt to use the parameter values that are similar to the real values. The main parameter variations map according to the work point variation shown in figure 2. In figure 2, τ_e (the sensor time constant), τ_d (the transport delay), f_α (a fraction of the injected fuel that enters the cylinder directly in each cycle) and f_β (a fraction of the fuel puddle that evaporates and enters the cylinder in each cycle) have been shown respectively. Variations of these parameters can easily be seen.

3. Model based predictive controller using wavelet neural network and state estimator

As A/F ratio control is a servo control problem and the plant does not have any natural integral loop, an external integral loop must be considered in the controller [5]. In our simulations, we have used a servo estimator as an alternative for comparison of controller performance. In this method, an ELS (Extended Lease Square) technique is used for identification of parameters of transport function.

The other control method that is used here is wavelet neural network. The learning capability and direct computation of work point dimensions using wavelet network are the main advantages of this method. But some prepared data as air mass map that is very useful, wouldn't be possible and whereas learning of this lack is difficult for wavelet neural network in part of work point space. Therefore a method that employs both the wavelet neural network and prepared data is sought. A good approach is applying a wavelet neural network and a plant model with constant and proper parameter values. For the air mass parameter, it is possible to use the prepared map. It is expected that this model have a partial convergence with the perfect model at critical work points. Applying a wavelet neural network, the gap between the desired control and the real control will be compensated and learned easily. In other words, applying a state estimator, the uncertainty will be reduced and a Wavenet will be more capable of learning the plant and the inverse plant map. In figure 2 a block diagram of the controller schema is shown.

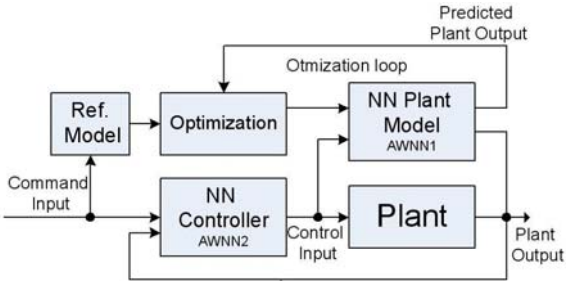

Figure2: A block diagram of the controller scheme

3.1. Designing an estimator

We consider A/F ratio control as a servo control problem in which because of using a Wavenet, an external loop is not utilized for rejecting steady state errors. Consequently the signal control is defined as:

$$u = -k_x (X - X_r) + u_{ss} \tag{7}$$

Here k_x is the state feedback gain, X_r is the reference state vector and u_{ss} is the steady state control effort and also we know the output signal must be constant at $y_r = 1$. From the reference signal y_r, the u_{ss} and X_r could be calculated as:

$$u_{ss} = (C*(I-G)^{-1}*H)^{-1}*y_r \tag{8}$$

$$X_r = (I-G)^{-1} H * u_{ss} \tag{9}$$

The open loop transfer function has two stable zeroes and four stable poles at $z = 1 - f_b, 0, 0, \gamma_0$ we define k_x such that the two zeroes are eliminated by the pole placement design method and the two other poles are placed at $z = 0.25 \pm .2j$. In order to estimate the states, full order estimator is used. For the estimator structure we use standard form. :

$$X = G\hat{X} + Hu + k_e(y - \hat{y}) \tag{10}$$

where k_e is the estimator gain vector since the roots of the estimator error characteristic equation is placed at $z = 0, 0, 0.25 \pm 0.2$.

3.2. Wavenet

The wavenet algorithms consist of two processes: the construction of networks and the minimization of error. In the first process, the network structure applied for representation of a given function is determined by using wavelet analysis. The network gradually selects functions in hidden units to effectively and sufficiently cover the time-frequency region occupied by a given target. Simultaneously, the network parameters are updated to preserve the network topology and take advantage of the later process. In the second process, the approximations of instantaneous errors are minimized using an adaptation technique based on the LMS algorithms. The optimization rule is only applied to the hidden units where the selected point falls into their windows. Therefore, the learning cost can be reduced. [11, 12] The *Wavenets* architecture employed in this paper has been shown in figure 3.

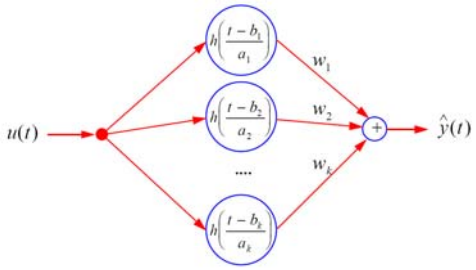

Figure 3: A Wavenet architecture schema

Approximates any desired signal $y(t)$ by generalizing a linear combination of a set of daughter wavelets $h_{a,b}(t)$, where $h_{a,b}(t)$ is generated by dilation, *a*, and translation, *b*, from a mother wavelet $h(t)$: $h_{a,b}(t) = h((t-b)/a)$ with the dilation factor $a > 0$.

The inversion formula [3] cannot be expressed directly by finite neural networks, but can be approximately realized using neural networks topology with finite number of hidden units. This is so because most targets are restricted in both time and frequency domains. Assuming that the network output function satisfies the admissibility condition and the network sufficiently approximates the target, i.e., the time-frequency region is effectively covered by their *K* windows, approximated signal of the network $\hat{y}(t)$ can be represented by the below equation where *K* is a number of windowing wavelets, and w_k are the weight coefficients. [13, 9]:

$$\hat{y}(t) = u(t)\sum_{k=1}^{K} w_k h_{a_k,b_k}(t)$$

3.3. Model based predictive controller

The use of MPC algorithm, requires defining, the following that are based on plant model. These include: a) cost function for optimization, b) a model for prediction and c) receding horizon to apply control derived by MPC. Regarding the order of the plant model and the number of zeroes, we can define the output signal as follows:

$$y(k) = F_1(y(k-1), y(k-2), y(k-3), y(k-4), u(k-2), u(k-3), u(k-4), n(k), \theta(k)) \tag{11}$$

It is clear from (11) that the plant has a delay of two and we can define the controller output as the following:

$$u(k) = F_2(y(k+2), y(k+1), y(k), y(k-1), y(k-2), u(k-1), n(k), \theta(k)) \tag{12}$$

Using (11) and replacing the future output signals with the current and previous control and output signals using Eq. (12), the above function can be written as:

$$u(k) = F_3\big(y(k+2), y(k-1),..., y(k-3), u(k-1),..., u(k-4), y(k-4), n(k), \theta(k), n(k+1), \theta(k+1), n(k+2), \theta(k+2)\big) \quad (13)$$

Considering (13), it is evident that the work point dimensions at the two future cycles have contributed to the current control signal so it is not possible to arrive at an inverse plant model and use it in the Wavenet unless a prediction is done.

$$u(k) \cong F_3\big(y(k-1), y(k-2), y(k-3), y(k-4), u(k-1), u(k-2), u(k-3), u(k-4), n(k), \theta(k)\big) \quad (14)$$

This prediction is indeed a robust and conservative approach to deal with rapid and random variations of the work points. The applied Wavenet is a multi layer perception with 10 inputs in accordance with the arguments for equation (14). We select the number of hidden layers and neurons through trial and errors so that the cost function $e(k) = (y_r - y(k))^2$, $y_r = 1$ is always a minimum. Finally a two layers network with 15 neurons at the hidden layer was selected. The activating functions in the first layer are Morlet wavelet functions given by: $f(x) = \cos(\omega_0 x)\exp\big(-0.5x^2\big)$ and in the second layer a linear function is used. The weights for Network have been adjusted using back propagation algorithm. The algorithm assumes that the plant operates as a sameness function so we use:

$$\partial e^2 / \partial y \approx \partial e^2 / \partial u_n \quad (15)$$

4. Simulations

The first simulation is about the response of the system to sudden variations of the work point by applying a combination of an estimator and Wavenet. Figure 5 shows that work point variations include a throttle valve angle variation simultaneous with an engine speed variation. This simulation obviously shows that applying the combined method reduces both oscillations as compared with the estimator response as well as rejecting the disturbance faster than a Wavenet response. So the performance in the combined method is better than a single method. Both in the estimator servo control method and the combined method, the placed poles are identical. In the second simulation, assuming the estimated air mass is used i.e. $\hat{m}_a = 1.5 * m_a + 20\ (mg)$, the robustness of the methods under additive and multiplicative errors for air mass in the whole work point space is examined. Figure 6 indicates that the estimator method cause instability while the response of the combination method is stable and the A/F ratio control performs well. Indeed using both a Wavenet and an estimator facilitates the use of prepared simulation data with parameter values are close to the real values. Consequently, uncertainties are reduced. Hence, a Wavenet would be capable of learning the additional uncertainties more rapidly and easier Using Wavenet a higher degree of robustness against parameter errors is achieved.

5. Conclusion

A stochiometric ratio at $\lambda_s = 14.5$, provides an ideal combustion results. Precise control of the A/F ratio at the stochiometric level by means of a catalyst converter yields an effective reduction of the emissions. However, the parameter variation due to work point variations is the main barrier for achieving a desired control results. In this paper, it has been shown that using both a Wavenet and an estimator would be an excellent approach to solve this problem. In fact, this method facilitates the use of all existing information. Moreover, using a Wavenet, the robustness of this method against the error estimation of parameters is considerably high.

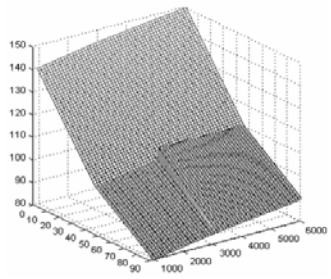

a1) τ_e (sensor time constant)

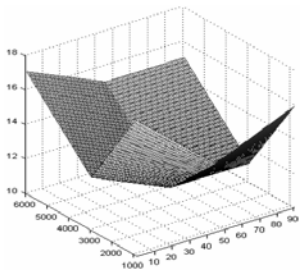

a2) τ_d (transport delay)

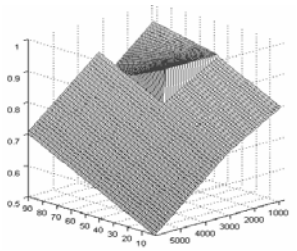

a3) f_α (fraction of injected fuel that enters the cylinder directly each cycle)

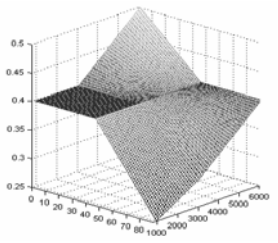

a4) f_β (fraction of fuel puddle that evaporates and enters the cylinder each cycle)

Figure 4 main parameters variations in work point space

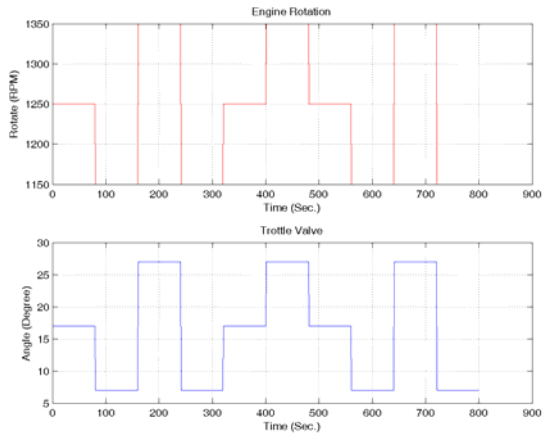

Figure 5 Engine speed and Throttle angle variations

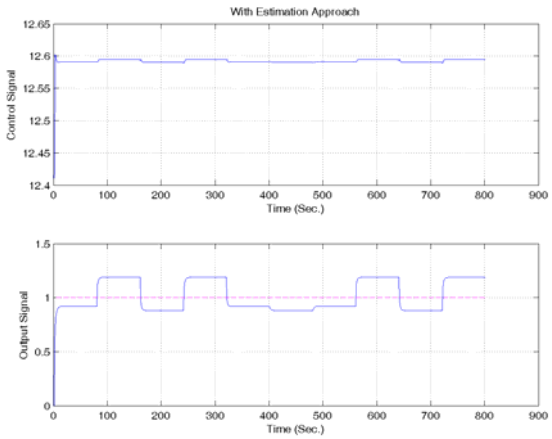

Figure 6 a) Engine speed and Throttle angle variations estimator method response

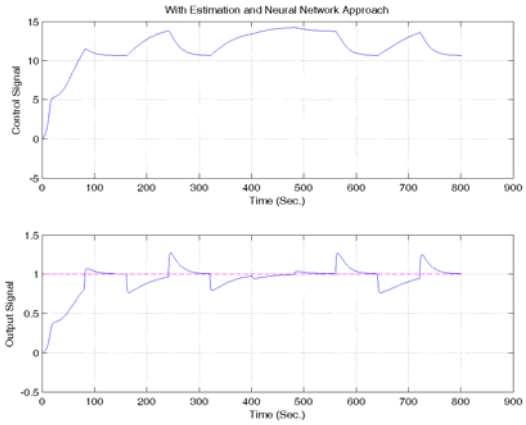

Figure 6 b) Engine speed and Throttle angle variations Neural Network method response

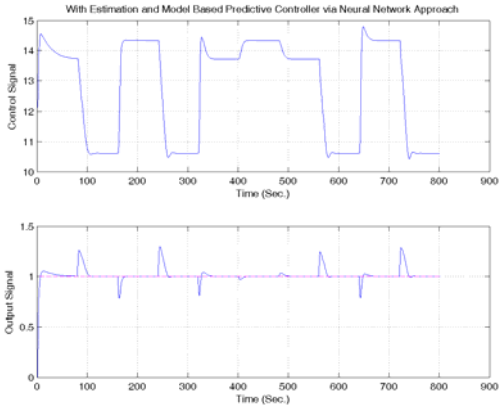

Figure 6 c) Engine speed and Throttle angle variations wavenets (with Morlet activation function) method response

6. References

[1] C.F. Chang, N.P. Fekete, A. Amustutz, J.D. Powell. Air Fuel Ratio Control in Spark Ignition Engines Using Estimation Theory. *IEEE*, March 1995

[2] J.D. Powell,N.P. Fekete, C.F. Chang. Observer Based Air-Fuel Ratio Control. *IEEE*, 1998

[3] Anand G., Gopinath S., Ravi M.R., Kar I.N., and Subrahmanyam J.P. Artificial Neural Networks for Prediction of Efficiency and NOx Emission of a Spark Ignition Engine. *SAE 2006 World Congress and Exhibition*, April 2006

[4] R. K. Young. *Wavelet Theory and Its Applications*, Kluwer Academic Publishers, Boston, MA, 1993

[5] N. Cesario, F. Taglialattela, and M. Lavorgna. SI engine control applications based on in-cylinder pressure signal processing. *Vehicle Power and Propulsion, 2005 IEEE Conference*, 7-9 Sept. 2005, pp. 11-20

[6] M.Won, S.B. Choi, J.K. Hedrick. Air-to-Fuel Ratio Control of Spark Ignition Engines Using Gaussian Network Sliding Control. *IEEE*, September 1998

[7] J.K. Pieper, R. Mehrotra. Air/Fuel Ratio Control Using Sliding Mode Methods. *ACC*, June 1999

[8] C. Allipi, C.D. Russis, V. Puri. A Fine Control Of The Air-to-Fuel Ratio With Recurrent Neural Networks *IEEE*, 1998

[9] I. Daubechies. The Wavelet Transform, Time-Frequency Localization and Signal Analysis. *IEEE Trans. Inform. Theory*, v36, n5, pp. 961-1005, Sept. 1990

[10] X. Ye and N. K. Loh. Dynamic System Identification Using Recurrent Radial Basis Function Network. *Proceedings of American Control. Conference*, v3. , pp. 2912-16, June 1993

[11] Q. Zhang and A. Benveniste. "Wavelet Networks. *IEEE Trans. Neural Networks*, v3, n6, pp. 889-98, Nov. 1992

[12] Y. Pati and P. Krishnaprasad. Analysis and Synthesis of Feedforward Neural Networks Using Discrete Affine Wavelet Transformation. *IEEE Trans. Neural Networks*, v4, n1, pp. 73-85, Jan. 1993

[13] A. N. Akansu and R. A. Haddad. *Multi-resolution Signal Decomposition: Transforms, Sub-bands, and Wavelets.* Academic Press, Inc., San Diego, CA, 1992